ISSN 1070-4272, Russian Journal of Applied Chemistry, 2009, Vol. 82, No. 2, pp. 209−212. © Pleiades Publishing, Ltd., 2009.
Original Russian Text © V.N. Viter, P.G. Nagornyi, 2009, published in Zhurnal Prikladnoi Khimii, 2009, Vol. 82, No. 2, pp. 215−219.

INORGANIC SYNTHESIS AND INDUSTRIAL INORGANIC CHEMISTRY

Synthesis and Study of Solid Acid Materials SnO_2/B_2O_3

V. N. Viter and P. G. Nagornyi

Shevchenko National University, Kiev, Ukraine

Received September 15, 2008

Abstract—SnO_2/B_2O_3 samples were produced by a reaction between $SnCl_4$, H_3BO_3, and $(NH_2)_2CO$ in a boiling aqueous solution. The Sn : B molar ratio in these samples was 1 : 1, 1 : 2, and 1 : 3. The phase composition and degree of crystallinity of these materials was studied. The surface acidity of the samples was analyzed by the method based on a temperature-programmed reaction of dehydration of 2-methyl-3-butyn-2-ol. Thermal transformations of SnO_2/B_2O_3 samples were examined by means of differential-thermal analysis.

DOI: 10.1134/S1070427209020086

A number of borates and materials containing boric anhydride serve as heterogeneous acid catalysts and catalyst supports. These compounds are of considerable interest for a wide variety of reactions. For example, the borates Al_2O_3/B_2O_3 catalyze dehydration of alcohols and, in particular, methanol [1]. $AlPO_4/B_2O_3$ and Al_2O_3/B_2O_3 samples exhibit activity in the reaction of skeletal isomerization of cyclohexene into methyl cyclopentenes, especially upon introduction of increased amounts of boric anhydride [2]. Tetralin has been successfully hydrogenated over a Pd–Pt bimetallic catalyst supported on amorphous aluminum borate. This catalyst shows good stability against presence of sulfur compounds and has a substantially higher selectivity compared with $Pd–Pt/SiO_2–Al_2O_3$, $Pd–Pt/\gamma\text{-}Al_2O_3$, and $Pd–Pt/SiO_2$ [3]. The catalytic properties of boron-substituted zeolites ZSM-5 and MCM-41 have been studied on the example of octene-1 isomerization. The incorporation of boron into these structures results in the formation of weak Lewis and Brønsted acid centers [4]. Use of the composite $NH_4–ZSM\text{-}5/B_2O_3$ made it possible to synthesize of *p*-xylene from toluene and methanol [5]. Mixed oxides $B_2O_3/TiO_2–ZrO_2$ catalyze the Beckmann rearrangement of cyclohexanone oxime into ε-caprolactam [6, 7]. Acid properties may also be expected for a number of other B_2O_3-containing systems and, in particular, SnO_2/B_2O_3.

The aim of this study was to obtain and examine the solid acid SnO_2/B_2O_3.

EXPERIMENTAL

The samples were produced from an aqueous solution of $SnCl_4$ (0.39 M), H_3BO_3, and $(NH_2)_2CO$. To a solution of $SnCl_4$ was added under heating a weighed portion of boric acid. After its complete dissolution, an excess of $(NH_2)_2CO$ was introduced. The Sn : B molar ratios were 1 : 1 (Sn1B1), 1 : 2 (Sn1B2), or 1 : 3 (Sn1B3). The reaction mixture was kept under weak-boiling conditions for 1 h. In the process, it was converted into a gel-like mass. The resulting product was dried at 120°C for 10 h. Then the samples were heated to 300–700°C at a rate not exceeding 7 deg min-1 and kept at a prescribed temperature for 1 h. The samples intended for thermogravimetric studies were dried at 100°C (without subsequent calcination).

Hydrated tin oxide $SnO_2 \cdot nH_2O$, produced by treatment of an aqueous solution of $SnCl_4$ with NH_3, was washed with water and dried. A mixture of aerosil and H_3BO_3 was pressed into pellets, which were calcined at 500°C for 1 h and used as reference. Acid catalysts ZrO_2/SiO_2 (Zr : Si molar ratios 33 : 67 and 25 : 75) were synthesized in two different ways: by the sol-gel method from $ZrO(NO_3)_2$ and $Si(OC_2H_5)$ and from NH_3, H_2SiF_6, and H_2ZrF_6. Mixed oxides ZrO_2/SiO_2 contain acid centers and exhibit activity in a number of reactions [8]. A superacid sample ZrO_2/WO_3 was obtained from aqueous solutions of ammonium metatungstate and zirconium nitrate (Zr : W molar ratio 8 : 1).

A thermogaphic analysis was made on a Q-1500 derivatograph in the temperature range 20–1000°C at a heating rate of 10 deg min-1. An X-ray phase analysis (XPA) was performed on a DRON-4-07 diffractometer ($Cu K_\alpha$ radiation). The specific surface area was found from adsorption of argon from an argon–helium mixture (5 vol % Ar) at a liquid-nitrogen temperature. Further, the

samples were heated to room temperature, and the amount of desorbed argon was measured with a catharometer and compared with that of a reference sample.

^{11}B NMR spectra were measured with a BRUKER AVANCE 400 spectrometer (working frequency 128.38 MHz) at room temperature in the magic-angle spinning mode (rotor 4 mm ZrO_2, frequency 10 kHz). $BF_3(C_2H_5)_2O$ served as external standard. IR spectra were recorded at room temperature with a Thermo Nicolet Nexus 670 spectrometer in KBr pellets.

The surface acidity of the samples was studied by the method of temperature-programmed reaction (TPR) of dehydration of 2-methyl-3-butyn-2-ol (MBOH) to 3-methyl-3-butene-1-yne (Mbyne) [9]. A 4-g portion of a sample was placed in a quartz reactor evacuated at 300°C. MBOH was adsorbed at room temperature with the subsequent evacuation of the reactor. Then the reactor

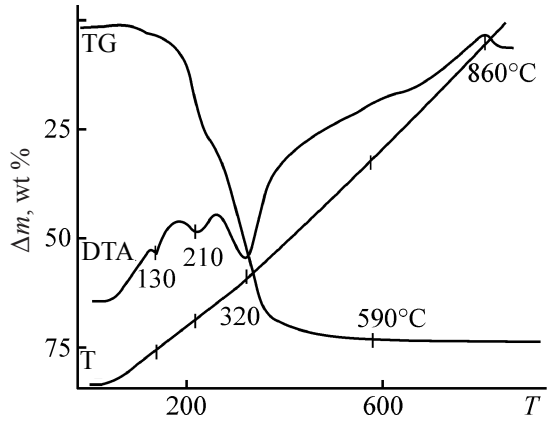

Fig. 1. Thermogram of Sn1B1 sample. (Δ*m*) Loss of mass and (*T*) temperature.

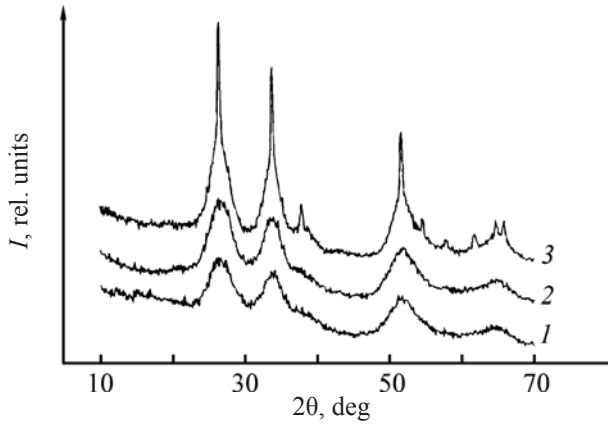

Fig. 2. X-ray diffraction pattern of Sn1B2 sample (CuK_α radiation) calcined at temperatures of (*1*) 300, (*2*) 400, and (*3*) 600°C for 1 h. (*I*) Intensity and (2θ) Bragg angle.

temperature was linearly varied from 20 to 260°C at a heating rate of 8 deg min^{-1}. The products obtained were analyzed with a mass spectrometer. Spectra of all the samples were measured under identical conditions.

The DTG curve of Sn1B1 sample (Fig. 1) shows three endothermic effects (at 130, 210, and 320°C) and one exothermic effect (around 860°C). According to TG data, the endothermic effects are associated with the loss of mass by a sample via release of H_2O, NH_3, and HCl. These gaseous products are formed in decomposition of boric acids, $SnO_2 \cdot nH_2O$, and NH_4Cl. The temperature of the minimum associated with the last endothermic effect (320°C) is close to the decomposition point of NH_4Cl (this substance is a product of the reaction between NH_3 and $SnCl_4$). The mass loss by Sn1B1 sample ends at a temperature of about 590°C and amounts to 74 wt %. The exothermic effect at 860°C is not associated with a change in the mass of a sample. In the case of pure $SnO_2 \cdot nH_2O$, the dehydration ends at 585–600°C.

X-ray diffraction patterns of Sn1B2 sample calcined at 300 and 400°C show broad reflections corresponding to tin dioxide (Fig. 2). This fact is due to presence of SnO_2 particles with low degree of crystallinity. On raising the thermal treatment temperature to 600°C, SnO_2 particles with both high and low degree of crystallinity are simultaneously present in the sample. This is indicated by the characteristic shape of reflections in the X-ray diffraction pattern (Fig. 2). A similar situation is observed for Sn1B1 and Sn1B3. At the same time, calcination of pure $SnO_2 \cdot nH_2O$ (at 500°C for 1 h) leads to formation of SnO_2 with a high degree of crystallinity. It has been noted previously that an exothermic effect peaked at 860°C is observed in the derivatogram of Sn1B1. Commonly, effects of this kind correspond to crystallization of substances from the amorphous phase. However, in the case under consideration, crystallization (and recrystallization) occurs in a ralatively wide temperature range. In addition, formation of crystalline SnO_2 is observed at temperatures substantially lower than 860°C.

Figure 3 shows how the specific surface area of samples depends on the temperature of their preliminary thermal treatment (heating rate not exceeding 7 deg min^{-1}). It can be seen that the specific surface area of Sn2B1 and Sn1B2 increases as the calcination temperature is elevated from 300 to 500°C, but steeply falls as this temperature is raised further to 600 and 700°C. A similar behavior is observed in Sn1B3. The increase in the specific surface of the samples on raising the calcination temperature is due to dehydration of boric acids and $SnO_2 \cdot nH_2O$ and to decomposition of NH_4Cl. The resulting structure is

constituted by SnO_2 (with low degree of crystallinity) and amorphous borate phase. The recrystallization and growth of SnO_2 crystals leads to a sharp decrease in the specific surface area.

As demonstrated by the TPR method, the reaction of MBOH dehydration occurs at the surface of Sn1B1, Sn1B2, and Sn1B3 materials calcined at 300–650°C, which points to the presence of acid centers. For all the samples (calcined at 400 or 500°C), the most intense formation of MBOH dehydration products is observed at temperatures of about 70–85°C (Figs. 4, 5). Under similar conditions, the ZrO_2/WO_3 acid catalysts have the highest activity at 80–100°C, and the superacid ZrO_2/WO_3, at about 40°C. Consequently, predominantly strong acid centers are present on the surface of Sn1B1, Sn1B2, and Sn1B3 samples calcined at 400 and 500°C. At the same time, these centers are not superacidic. In the TPR curves of Sn1B1 sample thermally treated at 300 and 650°C, peaks with a considerably lower intensity are observed at 100 and 80°C, respectively.

Conversion of MBOH into acetone on the surface of Sn1B1, Sn1B2, and Sn1B3 was not observed, which confirms the absence of basic centers [9]. At the same time, acetone formation occurred on the mixed oxide ZrO_2/SiO_2 (33 mol % ZrO_2).

The TPR curves of B_2O_3/SiO_2 (H_3BO_3/SiO_2 calcined at 500°C) have a single broad peak at 160°C (Fig. 4). Thus, the acid centers on the surface of this material have different strengths, but are mostly weak. In the case of $SnO_2 \cdot nH_2O$ calcined at 500°C, no MBOH dehydration was observed, which confirms the absence of acid centers. At the same time, it has been noted that MBOH isomerizes into 3-methyl-3-buten-2-one, which is due to the presence of amphoteric centers on the sample surface [9].

The above data unambiguously confirm that the acid properties of Sn1B1, Sn1B2, and Sn1B3 samples are due to the simultaneous presence of tin and boron oxides. Taken separately, these components contain only weakly acid (B_2O_3) or amphoteric ($SnO_2 \cdot nH_2O$) centers.

The ^{11}B NMR spectrum of Sn1B2 sample contains three peaks with chemical shifts δ 12.38, 7.23, and –2.14 ppm (Fig. 6). The first two lines are due to the presence of groups with a trigonal coordination of boron atoms (BO_3). The line with the chemical shift of –2.14 ppm is characteristic of BO_4 groups [10, 11]. IR spectra are also widely used to determine the coordination of boron atoms. At the same time, amorphous borates frequently simultaneously contain boron atoms with trigonal and tetragonal coordination, incorporated into

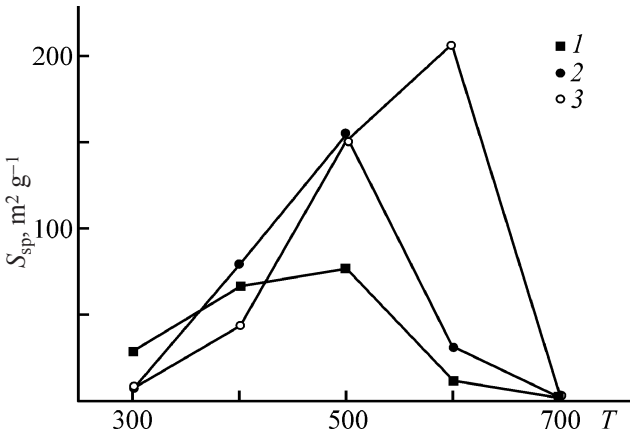

Fig. 3. Specific surface area S_{sp} of (*1*) Sn1B1, (*2*) SnB2, and (*3*) Sn1B3 samples vs. calcination temperature *T*. Calcination time 1 h.

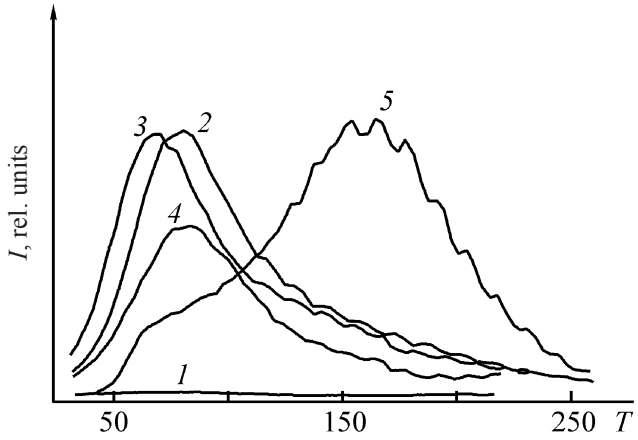

Fig. 4. TPR curves for MBOH dehydration to Mbyne on the surface of samples thermally treated at 500°C. Sample: (*1*) $SnO_2 \cdot nH_2O$, (*2*) Sn1B1, (*3*) Sn1B2, (*4*) Sn1B3, and (*5*) H_3BO_3/SiO_2. (*I*) Signal intensity and (*T*) temperature; the same for Fig. 5.

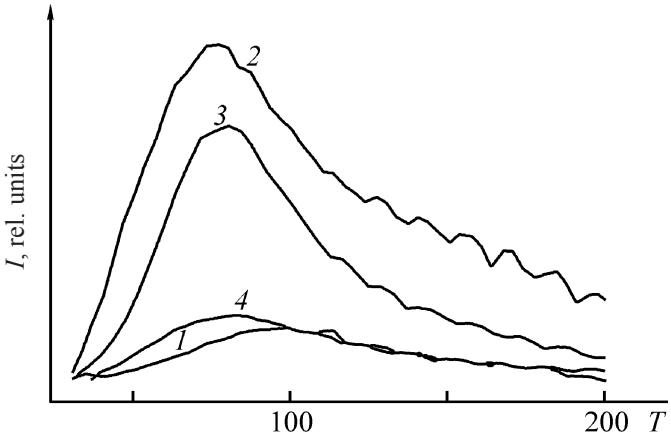

Fig. 5. TPR curves for MBOH dehydration to Mbyne on the surface of Sn1B1 sample calcined at (*1*) 300, (*2*) 400, (*3*) 500, and (*4*) 650°C.

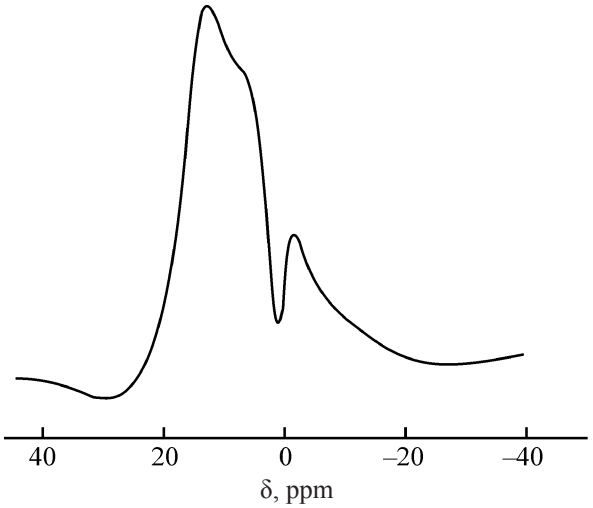

Fig. 6. 11B NMR spectrum (at magic-angle spinning) for Sn1B2 sample calcined at 500°C. (δ) Chemical shift.

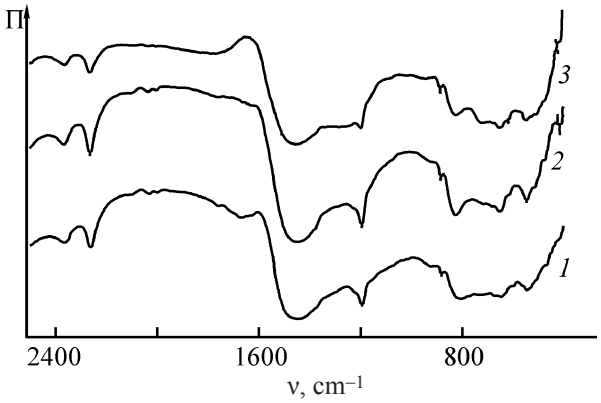

Fig. 7. IR spectra of Sn1B2 sample calcined at (*1*) 400, (*2*) 500, and (*3*) 700°C. (Π) Absorption and (ν) wave number.

complex low-symmetry polyanions. These factors make strict assignment of normal vibrations an exceedingly difficult task. At the same time, spectra of amorphous borates can be interpreted in terms of vibrations of the simplest groups: bridge groups B^{III}–O–B^{III} (absorption band 1300–1400 cm^{-1}), B^{III}–O–B^{IV} (1300–1100 cm^{-1}), B^{IV}–O–B^{IV} (900–1100 cm^{-1}); and terminal group B^{III}–O- (920–970 cm^{-1}) [12].

IR spectra of Sn1B2 sample calcined at different temperatures are shown in Fig. 7. The broad absorption band peaked at 1450 cm^{-1} can be assigned to vibrations of BO_3 groups connected by bridge bonds (B^{III}–O–B^{III}). At the same time, the band peaked at 1200 cm^{-1} can be attributed to vibrations of the bridge group B^{III}–O–B^{IV}. Consequently, the IR and NMR spectroscopic data confirm the simultaneous presence in the samples of trigonally and tetragonally coordinated boron atoms.

CONCLUSIONS

(1) Solid acid materials SnO_2/B_2O_3 were synthesized by a reaction between $SnCl_4$, H_3BO_3, and $(NH_2)_2CO$. The samples obtained contain SnO_2 (with varied degree of crystallinity) and an amorphous borate phase.

(2) The presence of predominantly strong acid centers on the surface of SnO_2/B_2O_3 was confirmed by the method of temperature-programmed reaction. This property is not manifested by separately taken components. The surface mostly contains weak acid centers for B_2O_3/SiO_2, and amphoteric centers, for pure SnO_2.

(3) The temperature maximum of MBOH dehydration for SnO_2/B_2O_3 is close to that for acid catalysts ZrO_2/SiO_2.

(4) According to IR and NMR spectroscopic data, SnO_2/B_2O_3 samples simultaneously contain boron atoms with trigonal and tetragonal coordination.

REFERENCES

1. Duarte de Farias, A.M., Lavogade Esteves, A.M., Ziarelli, F., et al., *Appl. Surface Sci.,* 2004, vol. 15, pp. 132–138.
2. Bautista, F.M., Campelo, J.M., Garcia, A., et al., *Appl. Catal. A: General*, 1998, vol. 170, pp. 159–168.
3. Yasuda, H., Kameoka, T., Sato, T., et al., *Appl. Catal. A: General*, 1999, vol. 185, pp. L199–L201.
4. Sundaramurthy, V. and Lingappan, N., *Microp. Mesop. Mater.*, 2003, vol. 65, pp. 243–255.
5. US Patent 7321072.
6. Mao, D., Lu, G., and Chen, Q., *Appl. Catal. A: General*, 2004, vol. 263, pp. 83–89.
7. Mao, D., Lu, G., and Chen, Q., *J. Mol. Catal. A: Chemical*, 2005, vol. 240, pp. 164–171.
8. Bosman, H.J.M., Kruissink, E.C., Vanderspoel, J., and Vandenbrink, F., *J. Catal*., 1994, vol. 148, pp. 660–672.
9. Kuśtrowski, P., Chmielarz, L., Boħek, E., et al., *Mater. Res. Bull.*, 2004, vol. 39, pp. 263–281.
10. Grimmer, A.-R., Muller, D., Gzel, G., and Kniep, R., *Fresenius J. Anal. Chem*., 1997, vol. 357, pp. 485–488.
11. Muller, K., Grimmer, A-R., Timper, U., et al., *Z. Anorg. Allgem. Chem.,* 1993, vol. 619, pp. 1262–1268.
12. Bobkova, N.M. and Khot'ko, S.A., *J. Appl. Spectrosc.*, 2005, vol. 72, pp. 853–857.